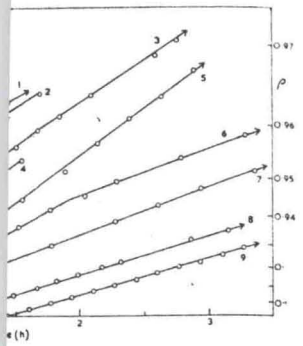

FIGURE 6
nents at 1300°C, pressure 5000 lb.in^{-2}.

two straight-line portions with
its: examples are Plots 3 and 6
change of gradient occurred at
ut 0·96, and a possible explana-
portion of the pore population
ng in an increase in the effective
The gradients for Plots 3 and 6
Table 1 are those of the first

ere sectioned and polished, using
d paste on successive lead laps.
cal microscopy. The remaining
clearly when the specimens were
ght using a × 140 oil immersion
res appeared as bright spots of
were too small to be optically
ere quite invisible under oblique
detected in this way: for such
vere actually diffraction patterns.
ined of the pore pattern below
each of the specimens: Figure 7
pe of photograph obtained.

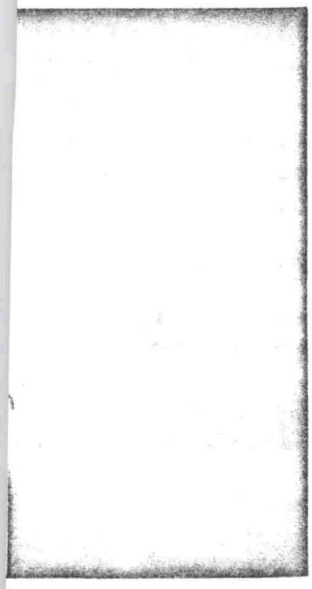

FIGURE 7
surface of a pressed specimen ($\rho = 0{\cdot}999$)

The number of pores visible in a fixed area (equivalent to about 50 μm^2) of each negative was counted. This number was, in each case, proportional to the number of pores lying within a layer of the specimen equal in thickness to the depth of field of the objective lens, and so was proportional to the pore density. Several pore counts were obtained for each specimen; average values are recorded in the last column of Table 1. If equations (4) and (5) are correct, then the gradient of the plot of $(\rho/P)^{\frac{1}{3}}$ *versus* time should be inversely proportional to the square of the pore separation (at any given temperature and pressure), i.e. the gradient raised to the power $\frac{3}{2}$ should be proportional to the pore density. In Figure 8 the gradients of the plots in Figure 6, raised to the power $\frac{3}{2}$, are plotted against the pore counts obtained from the photomicrographs. The points lie quite closely on a straight line through the origin, thus confirming the pore separation factor in Equation (4).

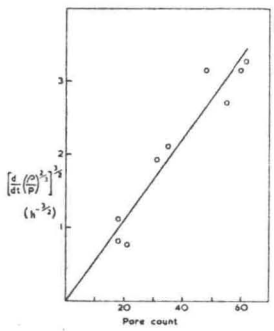

FIGURE 8
Correlation between the gradients of the plots in Figure 6 and pore densities.

7. CONCLUSIONS

The experiments described in Sections 5 and 6 confirm that the shrinkage rate of an alumina specimen during the final stage of densification ($\rho \gtrsim 0{\cdot}89$) is dependent on the applied pressure and on the mean pore separation in the manner predicted by Equation (4). In addition, the fact that straight-line plots of $(\rho/P)^{\frac{1}{3}}$ against time were obtained indicates that the predicted relationship between shrinkage rate and porosity is also correct.

In most experiments at constant load the gradient of the plot of $(\rho/P)^{\frac{1}{3}}$ against time was constant over a range of relative densities from well below 0·89 to about 0·96, indicating that no significant change in grain size or pore geometry was occurring. As has been mentioned, the gradient often decreased at a density of about 0·96, indicating some change in the effective pore geometry, but the experiments reported in Section 6 showed that the pore densities measured from the final compacts could be correlated with the shrinkage rates during the density range 0·90–0·94, which suggests that pores do not vanish altogether during densification, although they become very small before they stop shrinking. The observation that very high densities can be reached provided that sufficient pressing time is allowed suggests that pores do not become isolated from grain boundaries (at the temperatures and pressures used), for this would presumably hinder further shrinkage.

ACKNOWLEDGMENT

The Ministry of Technology is thanked for supporting this work.

MS RECEIVED 10/10/1968

REFERENCES

1. FRYER, G. M., *Trans. Brit. Ceram Soc.*, **66**, 127, 1967.
2. FRYER, G. M., *Trans. Brit. Ceram. Soc.*, **68**, 173. 1968.
3. See, for example, COBLE, R. L., "Mechanisms of Densification during Hot Pressing", in "Sintering and Related Phenomena"; Proceedings of a conference held at the University of Notre Dame, 1965 (Gordon and Breach, New York, 1967) p. 329.